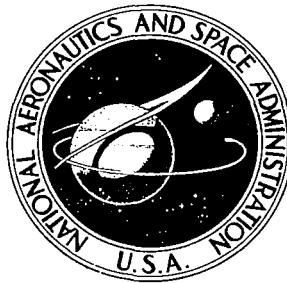


**NASA CONTRACTOR
REPORT**

NASA CR-1171



NASA CR-1171

0060334



LOAN COPY: RETURN TO
AFWL (WLIL-2)
KIRTLAND AFB, N. MEX

AN ALUMINUM NITRIDE MELTING TECHNIQUE

Prepared by
MATERIALS RESEARCH CORPORATION
Orangeburg, N. Y.
for Lewis Research Center

NATIONAL AERONAUTICS AND SPACE ADMINISTRATION • WASHINGTON, D. C. • SEPTEMBER 1968



0060334

NASA CR-1171

AN ALUMINUM NITRIDE MELTING TECHNIQUE

By Walter Class

Distribution of this report is provided in the interest of information exchange. Responsibility for the contents resides in the author or organization that prepared it.

Prepared under Contract No. NAS 3-10659 by
~~MATERIALS RESEARCH CORPORATION~~
 Orangeburg, N.Y.

for Lewis Research Center

NATIONAL AERONAUTICS AND SPACE ADMINISTRATION

For sale by the Clearinghouse for Federal Scientific and Technical Information
 Springfield, Virginia 22151 - CFSTI price \$3.00

FOREWORD

The work described herein was conducted at the Materials Research Corporation, under NASA Contract NAS3-10659 with John C. Sturman, Instruments and Computing Division, as Project Manager.

TABLE OF CONTENTS

<u>Section</u>	<u>Page</u>
I. INTRODUCTION.....	1
II. HIGH TEMPERATURE THERMOCHEMICAL CALCULATIONS.	3
III. APPARATUS AND EXPERIMENTAL PROCEDURE.....	10
A. Melting Apparatus.....	10
B. Specimen Preparation & Evaluation Methods	15
IV. RESULTS.....	18
A. Resistance Melting on Tungsten Filaments..	18
B. Resistance Melting Using Rhenium Filaments	18
C. Resistance Melting on Graphite Filaments..	21
D. Arc Melting on a Copper Hearth.....	23
V. INTERPRETATION AND DISCUSSION.....	26
A. Melting on Tungsten Filaments.....	26
B. Melting on Rhenium Filaments.....	27
C. Graphite Filaments.....	28
D. Arc Melting Results.....	29
VI. CONCLUSION.....	34
VII. REFERENCES.....	35

I. INTRODUCTION

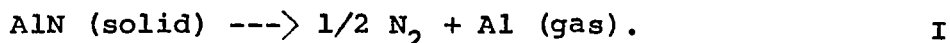
The achievement of stable melts of aluminum nitride would permit the application of conventional melt growth techniques to the single crystal preparation of this substance. This is of considerable interest because of the high temperature semi-conducting properties of this material. On this basis, a series of experimental studies was undertaken to evaluate the melting behavior of AlN and, in particular, to determine if pressures ≤ 200 atmospheres are sufficient to suppress the decomposition of this material at its melting point. Because the melting temperature of aluminum nitride is not known, this study also involved the determination of this temperature.

Two approaches were used in an attempt to achieve the above objectives. Firstly, a crucible melting operation was undertaken using resistively heated crucibles. Secondly, an arc melting operation was carried out on a cooled copper hearth in an effort to achieve uncontaminated melts of the aluminum nitride. As will become apparent, the crucible melting operation permitted the achievement of pressure stabilized melts. However, all the crucible materials examined (graphite, tungsten and rhenium) reacted with the molten aluminum nitride, thereby preventing an accurate determination of the melting point. The arc melting

operation, on the other hand, did not permit the achievement of stabilized melts because of the difficulty in achieving low power density arcs at the high pressures needed to stabilize the aluminum nitride melts.

II. HIGH TEMPERATURE THERMOCHEMICAL CALCULATIONS

The successful melting of aluminum nitride depends upon the suppression of the decomposition reaction which prevents the achievement of a chemically stable melt. A compilation of the thermochemical data regarding aluminum nitride is given in Tables I and II. These values are extracted from the JANAF thermochemical tables (1). From these data and other experimental results (2,3,4), there is little doubt that aluminum nitride decomposes by the reaction



The attached thermochemical tables therefore supply the necessary information to arrive at an estimate of the decomposition pressure of this material. This decomposition pressure can be calculated from the thermodynamic relationship:

$$\Delta F^\circ = -RT \ln K \quad (1)$$

where ΔF° is the free energy change of the reaction when all the products are in their standard states, R is the gas constant, T is the absolute temperature, and K is the equilibrium constant of the reaction. The free energy change is defined by the operation

$$\Delta F^\circ = (\text{sum of product free energies}) - (\text{sum of reactant free energies})$$

for a reaction of the above type in which a pure solid or liquid substance decomposes into two gaseous species, the equilibrium constant has the most general form

$$K = \frac{\left(\frac{f_{N_2}^*}{f_{N_2}^\circ} \right)^{1/2} \cdot \left(\frac{f_{Al}^*}{f_{Al}^\circ} \right)}{A_{AlN}^* / A_{AlN}^\circ} \quad (2)$$

where $f_{N_2}^*$ is the fugacity of nitrogen at the given pressure;
 $f_{N_2}^\circ$ is the fugacity of nitrogen in the standard state,
 f_{Al}^* and f_{Al}° are the corresponding fugacities for the aluminum vapor;

A_{AlN}^* and A_{AlN}° are the activities of the pure aluminum nitride at the corresponding given and standard states.

In the particular case here under consideration, none of the constituents are in their standard states, which are defined as:

- (1) For the solid - the pure substance at one atmosphere pressure. ($A^\circ = 1$ in this state.)
- (2) For the gases - the pure gas at unit fugacity; for an ideal gas the fugacity is unity when the pressure is 1 atmosphere, and the fugacity is numerically equal to the gas partial pressure (in atmospheres) at all pressures.

However, standard free energy values permit the calculation of equilibrium values of K and, hence, the decomposition pressure,

for any state provided that the appropriate fugacity and activities can be determined.

On this basis, if one assumes that the aluminum and nitrogen vapors behave ideally (recalling that $f_{N_2}^\circ = P_{N_2}^\circ = 1 \text{ atm}$, and $f_{Al}^\circ = P_{Al}^\circ = 1 \text{ atm}$), then K of Equation 2 becomes

$$K = \frac{\left(P_{N_2}\right)^{1/2} \left(P_{Al}\right)}{A_{AlN}^*} \quad (3)$$

where P_{N_2} and P_{Al} are the respective nitrogen and aluminum pressures in atmospheres.

The assumption of ideal behavior for nitrogen gas under these experimental conditions (high temperatures and gas pressures) is reasonable. The ratio of fugacity to pressure for nitrogen is .967 at 100 atmospheres and .971 at 200 atmospheres, and 273°K (5). Thus, even at room temperature, this ratio is very close to unity which corresponds to ideal behavior. At the high temperatures here under consideration, the departure of this ratio from unity should be negligible. Similarly, the aluminum vapor should behave in an ideal fashion at the high temperatures here under consideration.

Finally, it can be stated that the activity of the pure AlN is virtually equal to unity at the pressures used here. This may be seen from the fact that the activity of a pure substance varies

with the pressure according to the equation

$$\frac{dF}{dP} = RT \frac{d \ln a}{dP} = V \quad (4)$$

where V is the molar volume of the substance.

The integration of this equation requires a functional expression relating the molar volume to the pressure. This is obtained from the equation

$$\beta = - \frac{1}{V} \left(\frac{\partial V}{\partial P} \right)_T \quad (5)$$

where β is the isothermal compressibility of the aluminum nitride.

On this basis, Equation 3 may be integrated between the standard pressure (1 atm) and the actual pressure (200 atm) to arrive at an expression for the activity at this pressure. Thus

$$\ln a_{(200 \text{ atm})} = - \frac{1}{RT \beta} (V_{200 \text{ atm}} - V_{1 \text{ atm}}) \quad (6)$$

Now most solids have isothermal compressibility values equal to approximately $10^{-12} \text{ cm}^2/\text{dyne}$. Using this value and an atmospheric molar volume of 12.8 cm^3 , then gives at 3000°K

$$\begin{aligned} \ln a_{(200 \text{ atm})} &= -1.07 \times 10^{-2} \\ a_{(200 \text{ atm})} &= .999 \end{aligned}$$

Thus a value of unity substituted into the denominator of Equation 3 is justified. With the above substitutions, Equation 3 becomes

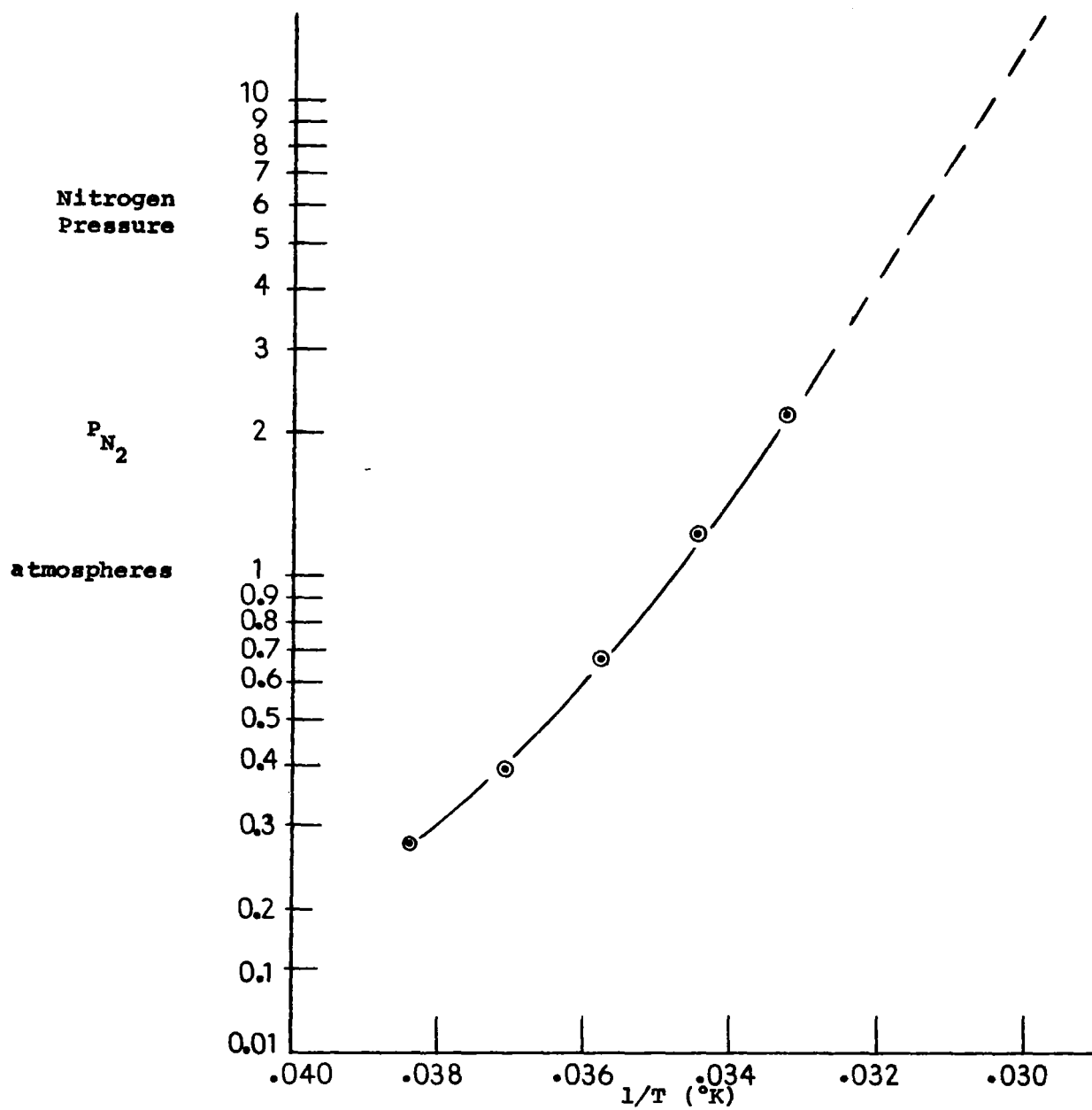
$$K_P = (P_{N_2})^{1/2} \cdot (P_{Al}) \quad (7)$$

Using this data and further recalling that if the vapors behave in an ideal manner

$$P_{N_2} = 1/2 P_{Al} \quad (8)$$

then permits the calculation of the equilibrium nitrogen pressure over solid AlN at different temperatures. It is further noted that this is also the equilibrium vapor pressure over liquid AlN at its melting point. Equations 7 and 8 used in conjunction with Table I then give the desired decomposition pressure values. It is noted that the values in Table I relate to the formation of AlN which is the reverse of reaction I. Thus, the figures on the table must be reversed in sign to give the proper calculated decomposition pressures. The results of these calculations are given in Figure 1 which is a plot of $\log P_{N_2}$ vs $1/T$. The extrapolation of this data to 3273°K gives a decomposition pressure of 10 atm nitrogen at this temperature. The total decomposition pressure is therefore approximately thirty atmospheres on this basis.

Using the tabulated values of K_p and an extrapolated value of $K_p = 1.801$ at 3273°K, then permits the calculation of the aluminum vapor pressure at a nitrogen pressure of 100 atm (a value typically applied in the experimental program). Such a calculation then gives aluminum vapor pressures of .65 and 6.3 atm at respective temperatures of 3000°K and 3273°K.



Aluminum Nitride Decomposition Pressure as a Function of Temperature

Figure 1

From these calculations it would appear that aluminum nitride can be stabilized in the environmental conditions supplied by the high pressure furnace used in these studies. As shall be described, this furnace was capable of providing temperatures up to 3000°C at a maximum pressure of 200 atmospheres.

III. APPARATUS AND EXPERIMENTAL PROCEDURE

A. Melting Apparatus

All the melting attempts were carried out in an autoclave designed to contain a gas pressure of 200 atmospheres. The gas was supplied from commercially available cylinders filled to 6000 psi. For the most part, this autoclave was pressurized with either pure nitrogen, nitrogen-hydrogen, or nitrogen-argon gas mixtures. The autoclave was equipped with a water-cooled coaxial power feed-through which served to supply RF power for the crucible melting operations, and DC power for the arc melting operations. In addition, another feed-through was supplied through which mechanical motion or additional electrical power could be supplied. Finally, the autoclave was equipped with a fused quartz window to permit visual observation of the melting operation as well as temperature measurement. A view of the autoclave is given in Figure 2, showing the window position. It is noted that the central portion of the autoclave was water cooled to prevent overheating from the pronounced convective heat transfer which occurred at these pressures.

The crucible melting operations were carried out by means of a dual element furnace which was mounted directly to one end plate of the autoclave. This furnace consisted of an inductively heated graphite sleeve within which a resistively heated filament

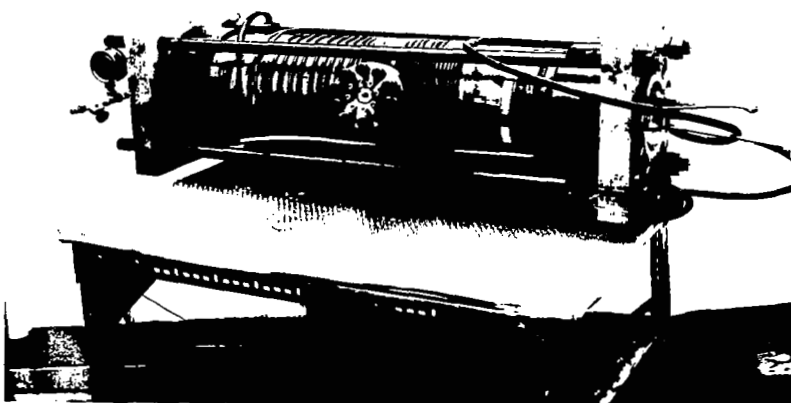


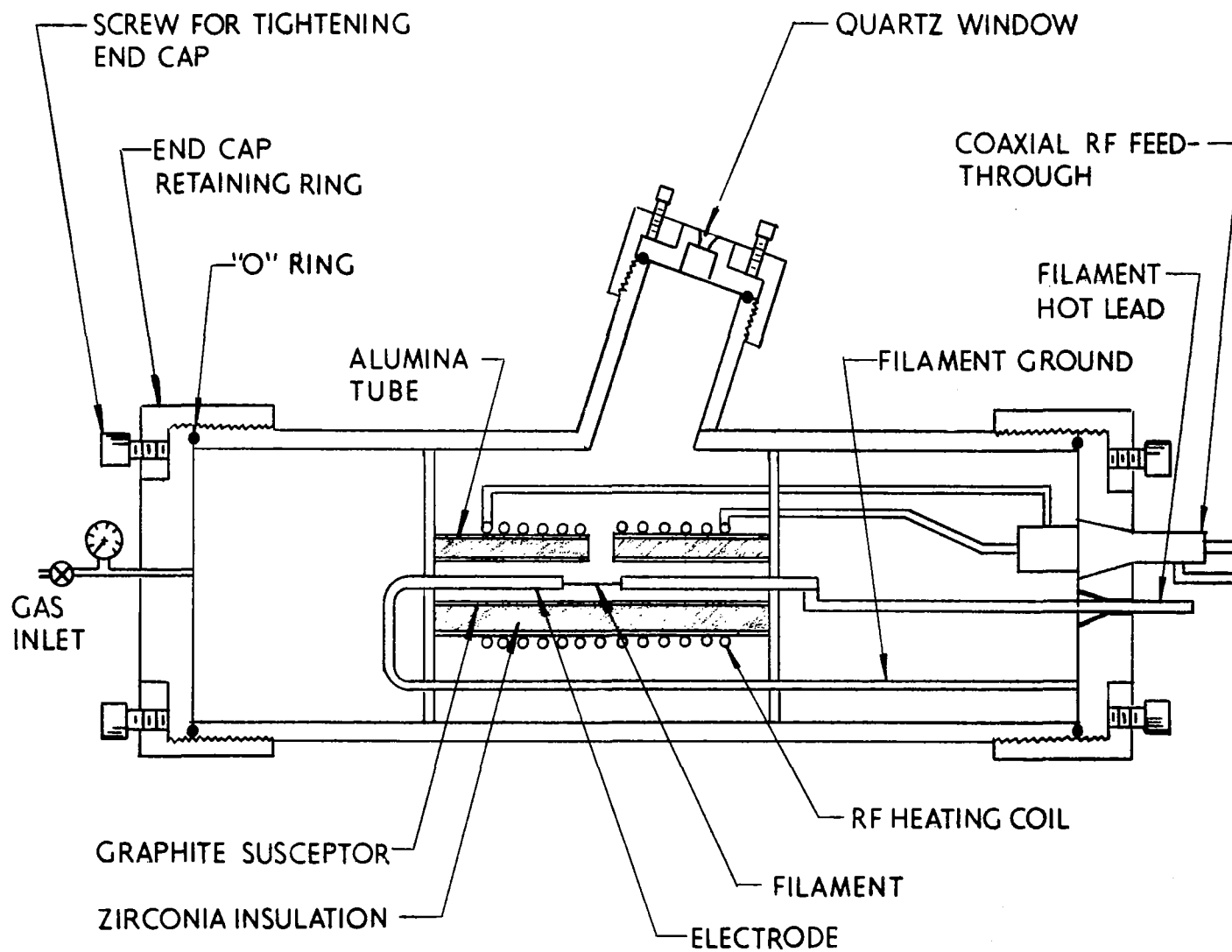
Figure 2
Autoclave Used in Aluminum Nitride
Melting Studies

was contained. The melting was accomplished by placing an aluminum nitride charge directly in contact with the filament which served to both melt and contain the charge. Filaments of tungsten, rhenium and graphite were utilized in this study. The dual element furnace was insulated with zirconia to prevent excessive heat losses from the inductively heated graphite sleeve. In addition, a port was provided through both the insulation and the graphite sleeve such that the filament could be viewed directly through the autoclave window. A general scheme of the furnace arrangement is given in Figure 3, while Figure 4 shows the furnace removed from the autoclave. Also visible is the coaxial power feed-through and the auxiliary filament power feed-through.

In practice, this furnace was capable of reaching graphite sleeve temperatures of 2000°C using a 15 KW output Lepel RF generator. Filament temperatures up to 2900°C were achieved with an auxiliary 9 KW AC supply.

The arc melting operation was accomplished by modifying the end cap of the autoclave initially used for resistance furnace mounting.

The coaxial feed-through was altered by attaching a tungsten "stinger" cathode in place of the RF coil. This stinger was made sufficiently long such that its tip was visible through the



AUTOCLAVE WITH ALN MELTING FURNACE

Figure 3

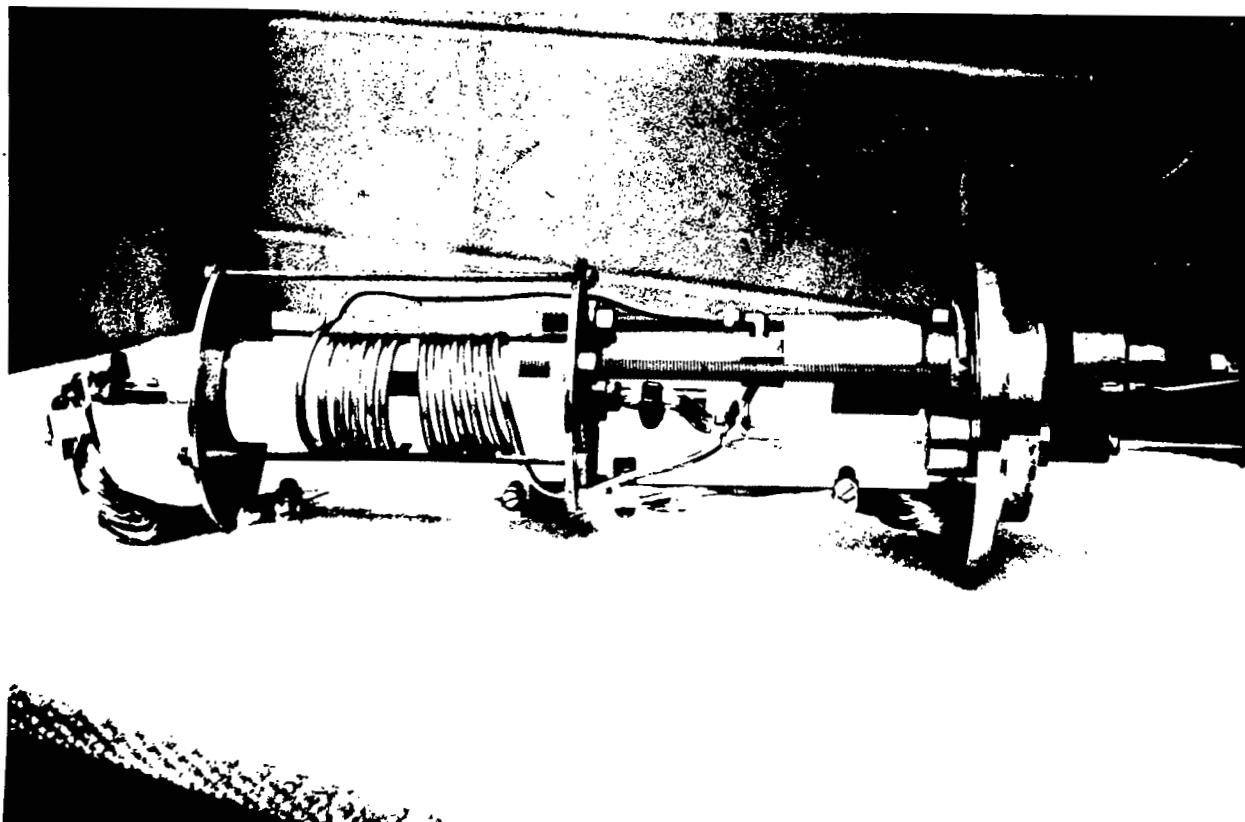


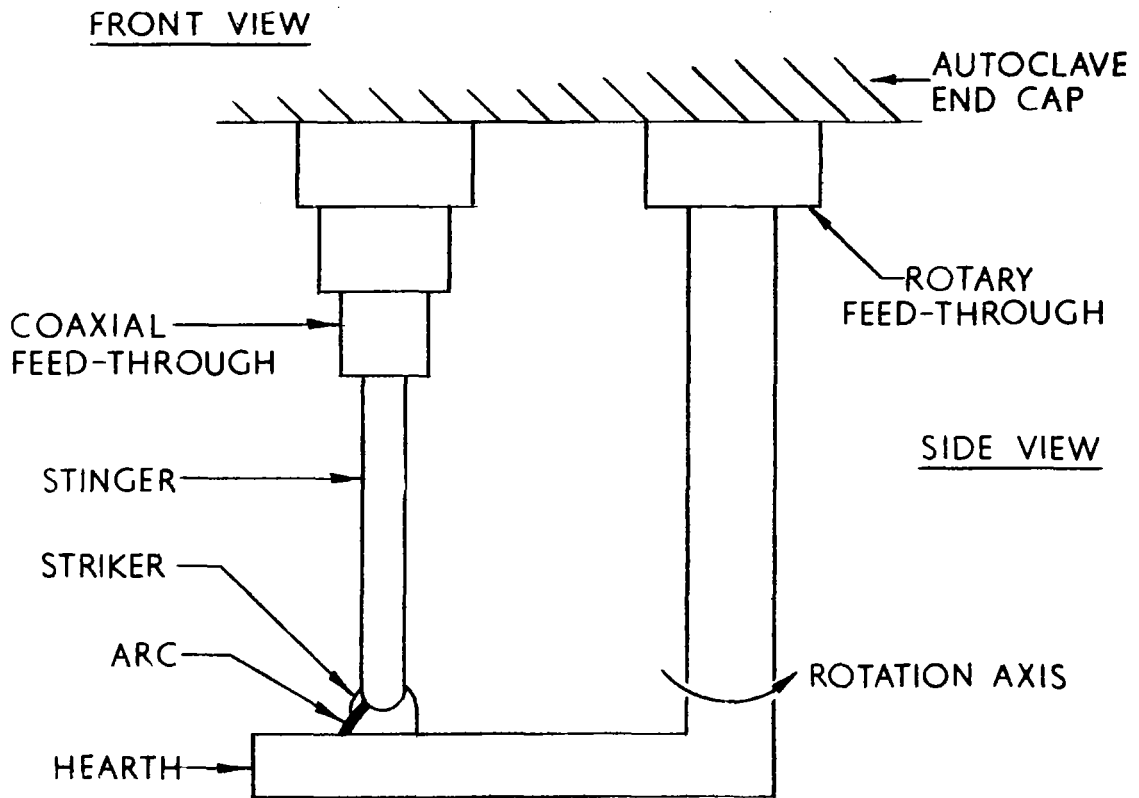
Figure 4

Aluminum Nitride Melting Furnace

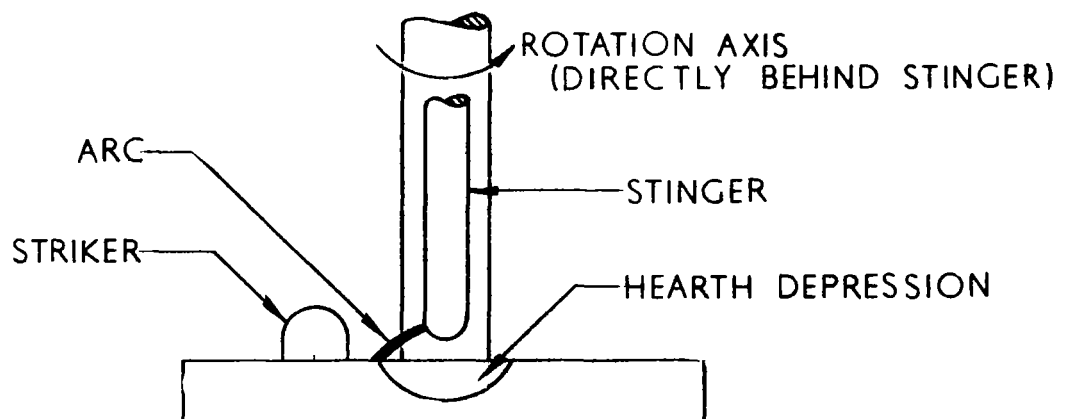
autoclave window. The autoclave was then mounted in a vertical position and a water-cooled copper hearth positioned directly below the stinger. Thus, both hearth and stinger tip could be viewed during operation. The copper hearth was mounted from an autoclave feed-through which permitted its rotation about an axis parallel to the stinger axis, but was not coaxial with the stinger. Thus, the hearth surface could be made to move in a plane perpendicular to the stinger axis, thereby permitting the initial striking of the arc and its transference to a position on the hearth where the aluminum nitride charge was located. The relative position of hearth, stinger and rotation axis are depicted in Figure 5. In practice, the aluminum nitride charge was placed within a hearth depression and an arc was struck by making contact between the stinger and a tungsten striker mounted in the hearth (see Figure 5). This arc was then transferred to the hearth and moved to the hearth depression where the aluminum nitride charge was located.

B. Specimen Preparation and Evaluation Methods

The aluminum nitride used in this study was Cerac Grade 1454 powder (-200 mesh) which typically contains 0.1% carbon as the primary impurity aside from unreacted aluminum metal. X-ray diffraction analysis of this material showed only the typical



SIDE VIEW (CORRESPONDS TO VIEWING DIRECTION THROUGH AUTOCLAVE WINDOW)



Schematic Illustration of Arc Melting Arrangement

Figure 5

aluminum nitride diffraction spectrum. The test specimens were formed from this material by pressing one-gram portions of the powder in a 3/8" diameter steel die at a pressure of 15,000 psi. The resulting pellets were approximately 3/8" high with a relative density of 75% of theoretical.

Throughout this study uncorrected pyrometer measurements were primarily used to determine the temperature. These results were calibrated in one instance by the use of a eutectic alloy of known melting point. Post-melt evaluation was accomplished by means of X-ray diffractometry, metallography and visual inspection.

IV. RESULTS

A. Resistance Melting on Tungsten Filaments

All attempts to melt aluminum nitride using tungsten filaments were terminated by failure of the filament at the point of contact with the aluminum nitride pellet. The maximum temperature, as measured by optical pyrometer (uncorrected), ranged from 2260°C to 2340°C.

Figure 6 shows a tungsten filament and the bottom of the aluminum nitride pellet after a run. A piece of tungsten filament became fused to the pellet, and the pellet surface is covered with a black, glassy material. Attempts to identify the residue from the tungsten filaments have been unsuccessful, only tungsten being definitely identified (Table IV).

B. Resistance Melting Using Rhenium Filaments

The attempts to melt aluminum nitride on rhenium filaments were terminated by filament melting at the point of contact with the aluminum nitride at temperatures of approximately 2700°C (optical pyrometer measurements). A temperature calibration of 2740°C was estimated by the formation of a molten tantalum-rhenium eutectic alloy drop prepared by placing a piece of tantalum on the rhenium filament. The rhenium failures appeared similar to the tungsten failures (see Figure 7). A black, glassy deposit was formed at the molten edge of the rhenium, and the aluminum nitride pellet did not melt.

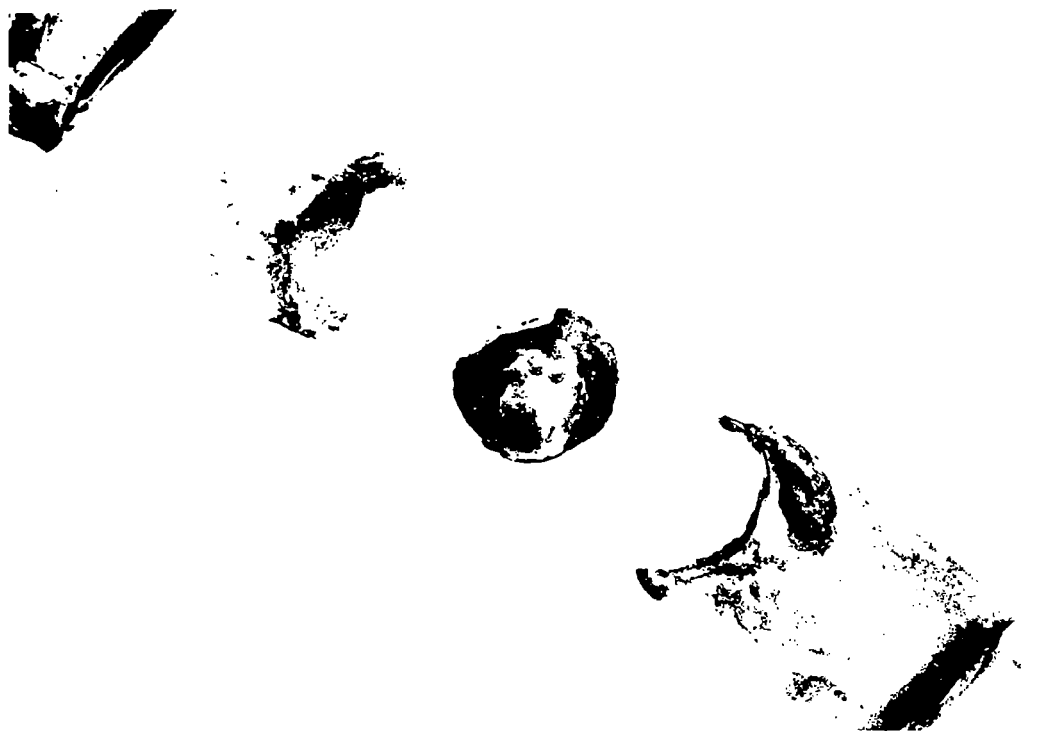


Figure 6

Tungsten Filament with AlN Pellet
After Melting Attempt

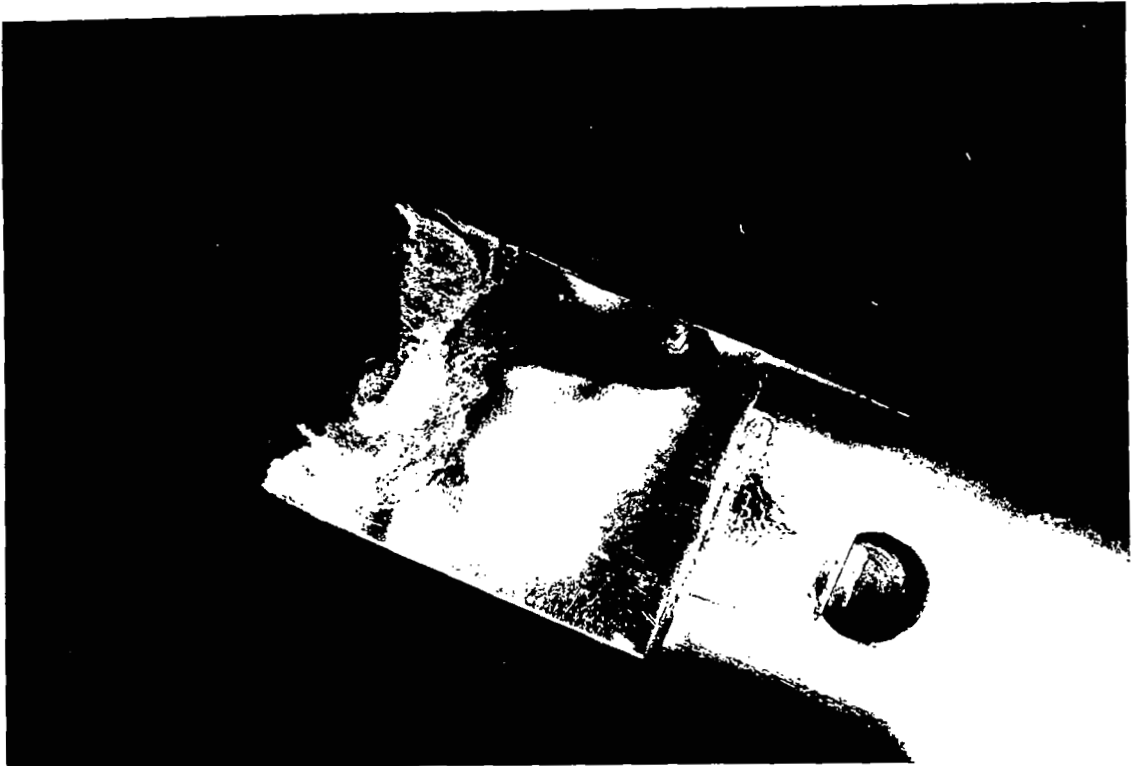


Figure 7

Rhenium Filament with Residue
After AlN Melting Attempt

X-ray diffraction analysis of the residue from the rhenium filaments showed only weak peaks associated with aluminum nitride and with rhenium (Table V).

C. Resistance Melting on Graphite Filaments

Two varieties of graphite filament were utilized in an attempt to melt aluminum nitride. These consisted of flat graphite strip filaments and filaments made from graphite tubes with a small radial viewing hole to permit melt inspection. The graphite was the most inert in the presence of aluminum nitride of all the materials tested.

Using the flat filament, a maximum temperature of 2750°C was achieved. At this temperature the aluminum nitride sintered very rapidly, exhibited considerable grain coarsening and showed rounding at sharp corners. The pellet had the overall appearance of having been raised close to its melting point. An X-ray diffraction analysis of the resulting specimen showed no contamination of the aluminum nitride (Table VI).

Using the graphite tube filaments, melting attempts were made at 2600°C and 2800°C at nitrogen pressures between 1500 psi and 3000 psi. The melting attempt at 2600°C and 1500 psi did not yield melting but the attempts at 2800°C with nitrogen pressures of 1500 psi and 3000 psi both yielded boules which were porous and had obviously melted. Figure 8 shows a typical

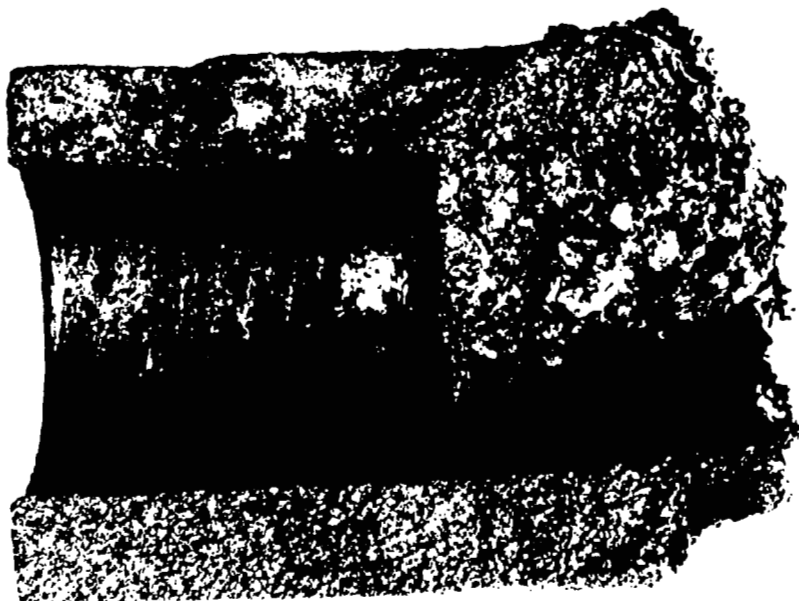


Figure 8

Section of Graphite Filament
Containing Aluminum Nitride Boule

melted boule. The original charge, consisting of the pressed pellets, adhered and conformed to the contour of the filament. Several voids were observed which were unmistakably bubbles at the filament-melt interface. The melted boules were black and mixed with graphite. Although they were brittle, individual crystallites within the boule were quite soft and easily scratched.

Once the melting point of the aluminum nitride was reached, the graphite filaments deteriorated very rapidly, failing within five minutes. The failure occurred at the area of contact with the aluminum nitride.

X-ray diffraction analysis of runs in which melting did not occur (Tables VII and VIII), showed only slight graphite contamination as shown by the very weak graphite peaks, whereas runs (Tables IX and X) in which melting did occur, were heavily contaminated by graphite, with graphite peaks more intense than the aluminum nitride peaks. One instance of aluminum carbide contamination was detected by X-ray diffraction. This result, however, could not be duplicated.

D. Arc Melting On a Copper Hearth

Whereas apparent melt stabilization could be achieved with the resistance melting on graphite filaments, no such stabilization could be achieved with the arc melting attempts, despite the fact

that stable arc could be attained at a 1500 psi gas pressure. The major difficulty with this process appeared to reside in the nature of the arc at the high pressures required for compound stabilization. At these pressures the impedance of the arc was rather high, a minimum of 60-80 volts being required to produce a stable arc. Furthermore, the diameter of the arc column became highly constricted at these pressures, resulting in very high current densities. Thus, despite rather low arc currents of 50 amperes, the arc current density and temperature were very high. Because of this, some difficulty was encountered with electrode stability. The tungsten stinger was frequently observed to undergo localized melting. A graphite stinger was also utilized with a resulting rapid vaporization of the material.

When such an arc made contact with the aluminum nitride, only highly localized heating of the material took place and this resulted in rapid evaporation of the material and its becoming deposited upon the interior walls of the autoclave in the form of a very low density, cotton-like deposit. This evaporation could be observed while the arc melting attempt was in progress.

Two experimental approaches were undertaken to minimize the detrimental effects of the high pressure arc constriction. Firstly, the nitrogen gas was mixed with argon. The addition

of argon, which is a low ionization potential gas, did not result in a considerable reduction in arc constriction and arc voltage. A 50% A-50% N₂ mixture at 1800 psi was found to give a stable arc. However, despite an arc column which was almost double the diameter of the corresponding pure nitrogen arc, the current densities were still considerably too high to give stable melting.

Another approach to the achievement of stable arc melting was to submerge both stinger and striker in an aluminum nitride charge to achieve submerged arc melting. This arrangement did not permit the achievement of a stable arc.

V. INTERPRETATION AND DISCUSSION

A. Melting on Tungsten Filaments

There is considerable evidence that the aluminum nitride reacted with the tungsten filament. The failure of the tungsten filaments at $\sim 2300^{\circ}\text{C}$ (which is approximately 1000°C below the tungsten melting point of 3380°C), most probably did not occur by localized melting of the filament as might occur at a higher temperature. Such failures can occur because of the much poorer thermal conductivity in that region of the filament covered by the aluminum nitride specimen. However, the appearance of the filament, as well as the fact that rhenium filaments (melting point 3100°C) withstood temperatures of 2700°C , suggests very strongly that a chemical reaction occurred to result in the filament failure. The X-ray diffraction trace indicates the formation of a compound which has not been successfully identified; however, it is not a commonly occurring compound of tungsten such as a nitride, carbide, aluminide or oxide.

There is further doubt that the filament failure occurred by some reaction with a constituent or impurity of the autoclave atmosphere. The regions of the filament not in contact with the aluminum nitride were clean and did not show signs of reaction.

B. Melting on Rhenium Filaments

The results of the melting attempts with rhenium were similar to those achieved with tungsten. The filaments have failed at a temperature of 2700°C and a similar residue was formed in these cases. Unfortunately, insufficient residue was formed to permit any accurate X-ray diffraction analysis. Thus, although no additional compound was detected, the appearance of the failed filament suggests very strongly that a reaction did occur.

The temperature of filament failure is estimated to be 2700°C by optical pyrometer measurements. However, at these temperatures the measurement of temperature became very difficult because of the severe optical distortions accompanying the heating at these high pressures. To calibrate the measurement, a small piece of tantalum was placed upon the filament and the solidification of the tantalum-rhenium eutectic droplet observed. The results are in agreement with the pyrometer measurement, within the experimental error.

In both the tungsten and the rhenium melting attempts, a 100 atm stabilization pressure was utilized. At this pressure, no apparent aluminum nitride evaporation was evident or observed by weight loss measurements.

C. Graphite Filaments

The graphite filaments proved to be the most inert to chemical attack by the aluminum nitride. The results of a run in which at a measured temperature of 2750°C and a nitrogen pressure of 1500 psi the aluminum nitride pellet showed evidence of sagging and surface glazing, represent the closest approximation to the melting point of aluminum nitride yet achieved. This temperature was determined by optical pyrometry and was subject to the previously mentioned errors induced by image distortion.

At this temperature and pressure the aluminum nitride did not show any evidence of decomposition, nor did it appreciably react with the graphite filament.

At the higher temperatures achieved in the tubular graphite filaments, the actual viewing of the aluminum nitride was not achieved, although a small axial hole was cut into the filament for this purpose. However, there is little doubt that molten AlN did exist for a short time period within the filament as evidenced by the coalescence of the original pellet charge into a single boule conforming to the filament contour. The temperature at which this process occurred was estimated to be in excess of 2800°C based upon power vs. temperature data extrapolated from lower temperatures. At the point where the melting took place,

the filament could not be distinguished from its lower temperature surroundings because of the severe convection currents which acted to distort the filament image. However, the melting power was well-known because of the rapid filament failure which occurred. Slightly lower power settings did not result in filament failure, nor did the aluminum nitride charge exhibit melting.

The porosity of the aluminum nitride, as well as the distinct evidence of graphite contamination, indicates that some vigorous agitation of the melt occurred at high temperatures. It appears that the agitation of the charge was the result of the chemical reaction which resulted in the failure of the filament. Some evidence of aluminum carbide formation was apparent from one melting attempt (see Table IX). However, this result could not be reproduced. It is not believed that the boule porosity resulted from a vigorous decomposition of the aluminum nitride because an increase in pressure from 1500 psi to 3000 psi did not have any effect upon this observed porosity. However, in view of the fact that the aluminum nitride melt could not be directly observed, this supposition is open to question.

D. Arc Melting Results

There is little doubt that part of the difficulty associated with the arc melting attempts can be attributed to the high arc

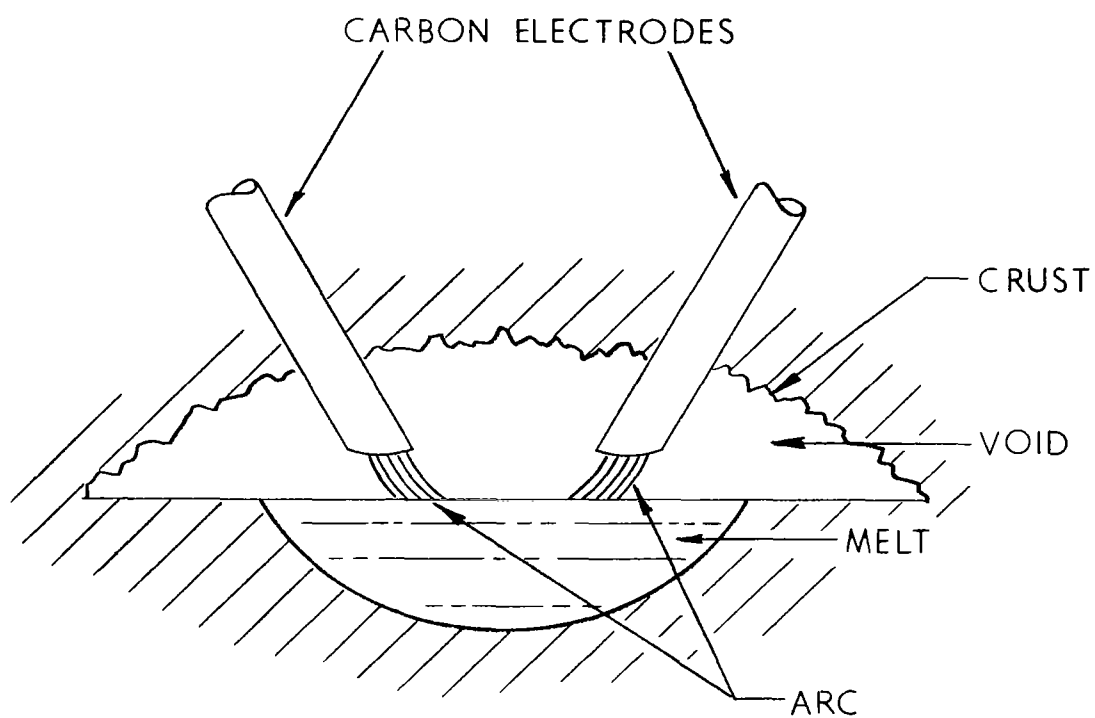
results in very high surface temperatures on the aluminum nitride. Thus, a considerably higher decomposition pressure results in the fact that a given stabilization pressure is no longer sufficient to stabilize the melt.

It is not believed, however, that this alone can account for the observed results because, if this were true, one would expect some localized sign of melting due to the fact that the high decomposition rate must come from a melt. No good evidence for any trace of melting could be observed. Thus, it appears that there is an apparent contradiction between the filament melting and the arc melting results. This contradiction can be explained upon the basis of the fact that the successful melting in the tubular graphite grid involved a situation in which the molten aluminum nitride was surrounded by its decomposition species in a confined space such that all reaction constituents are substantially at the same temperature. Thus, equilibrium conditions prevail and the stabilized melt is achieved. With arc melting, on the other hand, the melt is surrounded by gases at a much lower temperature and thus the aluminum and nitrogen vapor species recombine to form solid aluminum nitride, with the result that equilibrium is never achieved. Instead, a situation exists for the distillation of aluminum nitride away from the region of intense heating. This distillation can be very rapid because

firstly the decomposition pressures are high; hence, effusion from the hot region is rapid. Secondly, the massive convection currents present act to rapidly carry the decomposition products from the hot region. The distillation is accompanied by a heat sublimation loss from the hot region. Thus, a large heat input to the hot aluminum will result in rapid distillation. The heat of sublimation losses can then be sufficient to effectively prevent localized melting.

If this explanation of the arc melting process is correct, then a proper application of a submerged arc melting operation could give melting. Unfortunately, the experimental set-up was designed primarily for cold hearth melting and not for submerged arc melting, thereby preventing the achievement of a stable submerged arc.

The author recently became aware of an improved submerged arc melting process which may be applicable to the melting of aluminum nitride (6). With this method, a pair of carbon electrodes enters a bed of the material to be melted. A current is passed through the electrodes (in contact) to achieve high localized heating and partial melting. The electrodes are then separated and a small molten pool is formed which is contained within solid material of the same composition. The arrangement of electrodes and melt is depicted in Figure 9. From the figure



Possible Arrangement for Submerged Arc
Melting of Aluminum Nitride

Figure 9

it is seen that the material is confined within a small void which permits the attainment of equilibrium. Furthermore, the arc is transferred to the melt which is heated in part by Joule heating. Magnesium oxide has been melted successfully by this method with very little evidence of carbon contamination.

VI. CONCLUSION

On the basis of the foregoing, it is concluded that aluminum nitride cannot be melted in contact with graphite, tungsten or rhenium. It is estimated, however, that chemically stable melts of aluminum nitride can be achieved. The estimate of the melting point is difficult because of the presence of a chemical reaction between the aluminum nitride and its candidate crucible materials. However, the material does appear to melt within the limits of the 2750°-2850°C temperature range.

It may be further concluded that a nitrogen atmosphere at a pressure of 1500 psi is sufficient to suppress decomposition. This estimate, however, is subject to some question because of the presence of the chemical reaction.

VII. REFERENCES

1. JANAF Thermochemical Tables, prepared by Thermal Research Laboratory, Dow Chemical Co. Department of Commerce Publication PB-168370, August 1965.
2. W. Kleber and H.D. Witzke: Zeit. f. Krist. 116, 126 (1961).
3. J. Pasternak and L. Roskovcova: Phys. Stat. Sol. 7, 331 (1964).
4. P.O. Schissel and W.S. Williams: Bull. Am. Phys. Soc. II, 4, 139 (1959).
5. S. Glasstone: "Thermodynamics for Chemists", D. Van Nostrand Company, 1947, pg. 255.
6. J.W. Cleland: Symp. on Mass Transport in Oxides, National Bureau of Standards, A.D. Franklin, editor. To be published.

TABLE I
Aluminum Nitride (AlN)
(Crystal) Mol. Wt. = 40.988

T, °K.	cal. mole ⁻¹ deg. ⁻¹			kcal. mole ⁻¹			Log K _p
	C _p [°]	S [°]	-(F [°] -H ₂₉₈ [°])/T	H [°] -H ₂₉₈ [°]	ΔH _f [°]	ΔF _f [°]	
0	.000	.000	INFINITE	.925	- 74.795	- 74.795	INFINITE
100	1.360	.519	9.388	.887	- 75.205	- 73.187	159.942
200	4.613	2.455	5.399	.589	- 75.701	- 70.979	77.558
298	7.201	4.816	4.816	.000	- 76.000	- 68.595	50.279
300	7.225	4.861	4.816	.013	- 76.004	- 68.549	49.935
400	8.700	7.155	5.119	.814	- 76.149	- 66.038	36.080
500	9.701	9.210	5.736	1.737	- 76.204	- 63.503	27.756
600	10.439	11.048	6.471	2.747	- 76.207	- 60.962	22.204
700	10.915	12.696	7.245	3.816	- 76.188	- 58.423	18.240
800	11.255	14.177	8.020	4.926	- 76.166	- 55.887	15.267
900	11.495	15.518	8.780	6.064	- 76.155	- 53.352	12.955
1000	11.660	16.738	9.516	7.222	- 76.655	- 50.634	11.065
1100	11.769	17.855	10.224	8.394	- 78.577	- 47.835	9.504
1200	11.836	18.882	10.903	9.575	- 78.497	- 45.044	8.203
1300	11.876	19.831	11.554	10.760	- 78.417	- 42.260	7.104
1400	11.901	20.712	12.177	11.949	- 78.339	- 39.482	6.163
1500	11.923	21.534	12.774	13.140	- 78.262	- 36.709	5.348
1600	11.955	22.304	13.345	14.334	- 78.186	- 33.940	4.636
1700	12.000	23.030	13.894	15.532	- 78.110	- 31.178	4.008
1800	12.023	23.717	14.421	16.733	- 78.033	- 28.420	3.450
1900	12.035	24.367	14.927	17.936	- 77.957	- 25.664	2.952
2000	12.065	24.985	15.415	19.141	- 77.881	- 22.914	2.504
2100	12.092	25.575	15.885	20.349	- 77.804	- 20.169	2.099
2200	12.115	26.138	16.338	21.559	- 77.727	- 17.425	1.731
2300	12.135	26.677	16.776	22.772	- 77.649	- 14.687	1.396
2400	12.152	27.194	17.199	23.986	- 77.570	- 11.951	1.088
2500	12.165	27.690	17.609	25.202	- 77.491	- 9.218	.806
2600	12.183	28.167	18.006	26.420	- 77.412	- 6.490	.545
2700	12.199	28.628	18.391	27.639	- 77.333	- 3.763	.305
2800	12.215	29.072	18.765	28.859	- 147.807	.613	.048
2900	12.231	29.500	19.127	30.082	- 147.522	5.908	.445
3000	12.245	29.915	19.480	31.305	- 147.238	11.196	.816

Dec. 31, 1960; Dec. 31, 1961; Dec. 31, 1962

TABLE I. - Concluded.

ALUMINUM NITRIDE (AlN)

(CRYSTAL)

MOL. WT. = 40.99

$$\Delta H_f^0 = -74.8 \pm 0.3 \text{ kcal. mole}^{-1}$$

$$T_d = [2790^\circ\text{K}]$$

$$\Delta H_f^{298.15} = -76.0 \pm 0.3 \text{ kcal. mole}^{-1}$$

$$S_{298.15}^0 = 4.816 \text{ cal. deg.}^{-1} \text{ mole}^{-1}$$

Heat of Formation.

The selected heat of formation is the average of two independent calorimetric determinations. The heat of formation was reported to be $-76.5 \pm 0.2 \text{ kcal. mole}^{-1}$ and $-75.6 \pm 0.4 \text{ kcal. mole}^{-1}$. The former value was reported by C. A. Neugebauer and J. L. Margrave, *Z. Anorg. Allgem. Chem.* **290**, 82 (1957). The later value was reported by A. D. Mah, E. G. King, W. W. Weller, and A. V. Christensen, U. S. Bureau of Mines Report of Investigations 5716 (1961).

Vapor pressure measurements agree with the selected heat of formation. For instance $\Delta H_f^{298.15} = -75.5 \text{ kcal. mole}^{-1}$ for AlN(c) was calculated from the heat for the reaction $2\text{AlN(c)} \rightarrow 2\text{Al(g)} + \text{N}_2\text{(g)}$ and the heat of sublimation, $78.0 \text{ kcal. mole}^{-1}$, for Al(c). This heat of reaction was obtained from a third law calculation using JANAF values for the free energy functions and torsion effusion pressures measured by D. L. Hildenbrand and L. P. Theard, Aeronutronic Technical Report U-1497 (1961). Vapor pressure measurements with a microbalance in a vacuum system by L. H. Dreger, V. V. Dadape, and J. L. Margrave, *J. Phys. Chem.* **66**, 1556 (1962) agree with the selected $\Delta H_f^{298.15}$. When recalculated with the sublimation coefficient ($\alpha \approx 2.2 \times 10^{-3}$) reported by Hildenbrand and Theard, some of the Knudsen cell measurements by M. Hoch and D. White, "The Vaporization of Boron Nitride and Aluminum Nitride," ASTIA Unclassified Report 142616, October 29, 1956, agree with the selected heat of formation.

Earlier determinations of the heat of formation which apparently are in error are summarized by C. A. Neugebauer and J. L. Margrave (loc. cit.) and by L. H. Dreger et al. (loc. cit.).

Heat Capacity and Entropy.

The heat capacity and entropy were reported by A. D. Mah et al. (loc. cit.). They measured the low temperature ($51\text{--}298.15^\circ\text{K}$) and high temperature ($298.15\text{--}1800^\circ\text{K}$) heat capacities and extrapolated the heat capacity from 0 to 51°K using the T^3 law. A smooth extrapolation of the heat capacity was made from 1800° to 3000°K . The heat content of AlN(c) was recently determined from 300 to 1200°K by R. Mezaki, "Heat Contents of Inorganic Substances at High Temperatures," M. S. Thesis, University of Wisconsin (1961). The enthalpies reported by Mezaki are about 1% greater than those of Mah et al.

Decomposition Data.

P. O. Schissel and W. S. Williams, *Bull. Am. Phys. Soc.* **II**, **4**, 139 (1959) studied the vaporization of AlN with the mass spectrometer and detected only the gaseous species Al and N_2 . The temperature at which the ΔF_f^0 of AlN(c) and Al(g) were equal, 2788.9°K , was taken as the temperature of decomposition.

TABLE II

Aluminum Nitride (AlN)

(Ideal Gas) GFW = 40.9882

T, °K	gibbs/mol			kcal/mol			Log Kp
	Cp°	S°	-(G°-H° ₂₉₈)/T	H°-H° ₂₉₈	ΔHf°	ΔGf°	
0	.000	.000	INFINITE	- 2.106	104.024	104.024	INFINITE
100	6.957	42.840	56.950	- 1.411	104.266	102.056	- 223.043
200	7.079	47.683	51.242	- .712	104.176	99.853	- 109.114
298	7.444	50.573	50.573	.000	104.000	97.763	- 71.662
300	7.452	50.620	50.574	.014	103.996	97.724	- 71.192
400	7.838	52.818	50.871	.779	103.814	95.661	- 52.267
500	8.134	54.601	51.444	1.578	103.631	93.644	- 40.932
600	8.347	56.104	52.099	2.403	103.440	91.664	- 33.389
700	8.500	57.402	52.766	3.246	103.234	89.718	- 28.011
800	8.612	58.545	53.418	4.102	103.002	87.802	- 23.986
900	8.697	59.564	54.045	4.967	102.726	85.919	- 20.864
1000	8.763	60.484	54.644	5.840	99.879	84.251	- 18.413
1100	8.815	61.322	55.214	6.719	99.605	82.701	- 16.431
1200	8.858	62.091	55.755	7.603	99.329	81.176	- 14.784
1300	8.894	62.801	56.270	8.491	99.053	79.675	- 13.395
1400	8.925	63.462	56.760	9.382	98.775	78.195	- 12.207
1500	8.952	64.078	57.228	10.276	98.495	76.735	- 11.180
1600	8.976	64.657	57.674	11.172	98.214	75.293	- 10.285
1700	8.997	65.202	58.101	12.071	97.933	73.868	- 9.496
1800	9.017	65.717	58.510	12.971	97.651	72.462	- 8.798
1900	9.035	66.205	58.902	13.874	97.368	71.070	- 8.175
2000	9.052	66.668	59.279	14.774	97.084	69.694	- 7.616
2100	9.067	67.110	59.642	15.684	96.800	68.331	- 7.111
2200	9.082	67.533	59.991	16.592	96.516	66.980	- 6.654
2300	9.096	67.937	60.328	17.501	96.232	65.646	- 6.238
2400	9.110	68.324	60.653	18.411	95.948	64.323	- 5.857
2500	9.123	68.696	60.967	19.323	95.663	63.009	- 5.508
2600	9.135	69.054	61.271	20.236	95.379	61.710	- 5.187
2700	9.147	69.399	61.566	21.150	95.094	60.419	- 4.891
2800	9.159	69.732	61.852	22.065	94.800	59.170	- 4.681
2900	9.171	70.054	62.129	22.982	94.507	57.970	- 4.461
3000	9.182	70.365	62.398	23.899	94.213	56.821	- 4.249
3100	9.193	70.666	62.660	24.818	93.919	55.725	- 4.048
3200	9.204	70.958	62.915	25.738	93.625	54.682	- 3.854
3300	9.215	71.242	63.163	26.659	93.331	53.692	- 3.666
3400	9.226	71.517	63.405	27.581	93.037	52.754	- 3.482
3500	9.236	71.784	63.640	28.504	92.743	51.866	- 3.302
3600	9.247	72.045	63.870	29.424	92.449	51.026	- 3.126
3700	9.257	72.298	64.095	30.353	92.155	50.232	- 2.954
3800	9.267	72.545	64.314	31.279	91.861	49.482	- 2.785
3900	9.277	72.786	64.528	32.207	91.567	48.775	- 2.620
4000	9.287	73.021	64.737	33.135	91.273	48.110	- 2.458
4100	9.297	73.251	64.942	34.064	90.979	47.484	- 2.300
4200	9.307	73.475	65.143	34.994	90.685	46.897	- 2.145
4300	9.317	73.694	65.339	35.925	90.391	46.350	- 2.000
4400	9.327	73.908	65.531	36.858	90.097	45.841	- 1.860
4500	9.336	74.118	65.720	37.791	89.803	45.370	- 1.725
4600	9.346	74.323	65.905	38.725	89.509	44.937	- 1.594
4700	9.356	74.524	66.086	39.660	89.215	44.541	- 1.466
4800	9.365	74.721	66.264	40.596	88.921	44.182	- 1.342
4900	9.375	74.915	66.438	41.533	88.627	43.860	- 1.221
5000	9.385	75.104	66.610	42.471	88.333	43.574	- 1.102
5100	9.394	75.290	66.778	43.410	88.039	43.324	- 1.000
5200	9.404	75.472	66.944	44.350	87.745	43.109	- 0.900
5300	9.413	75.652	67.106	45.291	87.451	42.928	- 0.800
5400	9.423	75.828	67.266	46.233	87.157	42.781	- 0.700
5500	9.432	76.001	67.423	47.175	86.863	42.667	- 0.600
5600	9.441	76.171	67.578	48.119	86.569	42.586	- 0.500
5700	9.451	76.338	67.730	49.064	86.275	42.528	- 0.400
5800	9.460	76.502	67.880	50.009	85.981	42.491	- 0.300
5900	9.470	76.664	68.028	50.956	85.687	42.474	- 0.200
6000	9.479	76.823	68.173	51.903	85.393	42.477	- 0.100

Dec. 31, 1960; Mar. 31, 1964; Mar. 31, 1967

TABLE II. - Concluded.

ALUMINUM NITRIDE (AlN)

(IDEAL GAS)

GFW = 40.9882

Ground State Configuration [$1\Sigma^+$]

$$\Delta H_f^\circ = 104 \pm 20 \text{ kcal/mol}$$

$$S_{298.15}^\circ = [50.573] \text{ gibbs/mol}$$

$$\Delta H_f^\circ_{298.15} = 104 \pm 20 \text{ kcal/mol}$$

Electronic Levels and Quantum Weights

$\epsilon_1, \text{ cm}^{-1}$	g_1
0	1

$$\omega_e = [930] \text{ cm}^{-1}$$

$$\omega_e x_e = [6.9] \text{ cm}^{-1}$$

$$\sigma = 1$$

$$B_e = [0.6748] \text{ cm}^{-1}$$

$$\alpha_e = [0.0064] \text{ cm}^{-1}$$

$$r_e = [1.65] \text{ \AA}$$

Heat of Formation.

The heat of formation is calculated from the estimated ω_e and $\omega_e x_e$, using $D_0 = \omega_e^2 / 4\omega_e x_e$, as 89 kcal/mol. J. L. Margrave and P. Staphitanonda, J. Phys. Chem. 59, 1231 (1955) estimated values of the bond length as 1.23 - 1.65 Å and calculated from an ionic model D_0 values of 137 - 82 kcal/mol. Using an estimated bond length of 1.65 Å and a $D_0 = 87$ kcal/mol leads to $\Delta H_f^\circ_{298} = 104$ kcal/mol.

Heat Capacity and Entropy.

The bond length is estimated as 1.65 Å from a comparison with the bond lengths of SO, PO, SiO, AlO, MgO, S₂, SiS, AlS, PN, SiN, and the sums of covalent radii. This bond length is then used with Guggenheimer's Relation [K. M. Guggenheimer, Proc. Phys. Soc. (London), 58, 456 (1946)] to calculate a value for ω_e . By analogy with SiN(g) it is taken to closely approach the multiple bonding case, which gives $\omega_e = 960 \text{ cm}^{-1}$. The anharmonicity correction x_e is calculated by assuming the product $x_e \mu^{1/2}$ equal to that for AlO(g). The value of α_e is calculated using the relation:

$$\alpha_e = 6[(\omega_e x_e B_e^3)^{1/2} - B_e^2] / \omega_e$$

TABLE III

Aluminum (Al)

(Reference State)

T, °K.	cal. mole ⁻¹ deg. ⁻¹				kcal. mole ⁻¹			Log K _P
	C _P ^o	S ^o	-(F ^o -H ₂₉₈ ^o)/T		H ^o -H ₂₉₈ ^o	ΔH _f ^o	ΔF _f ^o	
0	0.000	0.000	INFINITE	-	1.094	0.000	0.000	0.000
100	3.116	1.650	11.529	-	.988	0.000	0.000	0.000
200	5.158	4.572	7.300	-	.546	0.000	0.000	0.000
298	5.820	6.769	6.769	-	0.000	0.000	0.000	0.000
300	5.826	6.805	6.769		.011	0.000	0.000	0.000
400	6.124	8.522	7.001		.608	0.000	0.000	0.000
500	6.402	9.919	7.449		1.235	0.000	0.000	0.000
600	6.716	11.114	7.963		1.891	0.000	0.000	0.000
700	7.012	12.172	8.490		2.578	0.000	0.000	0.000
800	7.318	13.128	9.011		3.294	0.000	0.000	0.000
900	7.636	14.008	9.518		4.041	0.000	0.000	0.000
1000	7.000	17.506	10.192		7.313	0.000	0.000	0.000
1100	7.000	18.173	10.888		9.013	0.000	0.000	0.000
1200	7.000	18.782	11.521		8.713	0.000	0.000	0.000
1300	7.000	19.342	12.101		9.413	0.000	0.000	0.000
1400	7.000	19.861	12.637		10.113	0.000	0.000	0.000
1500	7.000	20.344	13.135		10.813	0.000	0.000	0.000
1600	7.000	20.796	13.600		11.513	0.000	0.000	0.000
1700	7.000	21.220	14.036		12.213	0.000	0.000	0.000
1800	7.000	21.620	14.446		12.913	0.000	0.000	0.000
1900	7.000	21.999	14.834		13.613	0.000	0.000	0.000
2000	7.000	22.358	15.201		14.313	0.000	0.000	0.000
2100	7.000	22.699	15.550		15.013	0.000	0.000	0.000
2200	7.000	23.025	15.883		15.713	0.000	0.000	0.000
2300	7.000	23.336	16.200		16.413	0.000	0.000	0.000
2400	7.000	23.634	16.503		17.113	0.000	0.000	0.000
2500	7.000	23.920	16.794		17.813	0.000	0.000	0.000
2600	7.000	24.194	17.074		18.513	0.000	0.000	0.000
2700	7.000	24.458	17.342		19.213	0.000	0.000	0.000
2800	4.970	50.501	18.191		90.467	0.000	0.000	0.000
2900	4.971	50.675	19.308		90.964	0.000	0.000	0.000
3000	4.971	50.844	20.357		91.461	0.000	0.000	0.000
3100	4.971	51.007	21.343		91.958	0.000	0.000	0.000
3200	4.972	51.165	22.272		92.456	0.000	0.000	0.000
3300	4.973	51.318	23.150		92.953	0.000	0.000	0.000
3400	4.975	51.466	23.981		93.450	0.000	0.000	0.000
3500	4.977	51.610	24.768		93.948	0.000	0.000	0.000
3600	4.979	51.751	25.516		94.446	0.000	0.000	0.000
3700	4.982	51.887	26.227		94.944	0.000	0.000	0.000
3800	4.986	52.020	26.904		95.442	0.000	0.000	0.000
3900	4.991	52.150	27.549		95.941	0.000	0.000	0.000
4000	4.996	52.276	28.166		96.440	0.000	0.000	0.000
4100	5.002	52.399	28.755		96.940	0.000	0.000	0.000
4200	5.010	52.520	29.320		97.441	0.000	0.000	0.000
4300	5.019	52.638	29.861		97.942	0.000	0.000	0.000
4400	5.029	52.753	30.380		98.445	0.000	0.000	0.000
4500	5.041	52.867	30.878		98.948	0.000	0.000	0.000
4600	5.055	52.978	31.357		99.453	0.000	0.000	0.000
4700	5.071	53.086	31.819		99.959	0.000	0.000	0.000
4800	5.088	53.193	32.263		100.467	0.000	0.000	0.000
4900	5.108	53.299	32.691		100.977	0.000	0.000	0.000
5000	5.130	53.402	33.104		101.489	0.000	0.000	0.000
5100	5.154	53.504	33.503		102.003	0.000	0.000	0.000
5200	5.181	53.604	33.889		102.520	0.000	0.000	0.000
5300	5.211	53.703	34.262		103.039	0.000	0.000	0.000
5400	5.244	53.801	34.623		103.562	0.000	0.000	0.000
5500	5.280	53.897	34.972		104.088	0.000	0.000	0.000
5600	5.319	53.993	35.311		104.618	0.000	0.000	0.000
5700	5.361	54.087	35.640		105.152	0.000	0.000	0.000
5800	5.406	54.181	35.958		105.690	0.000	0.000	0.000
5900	5.456	54.274	36.268		106.233	0.000	0.000	0.000
6000	5.508	54.366	36.569		106.782	0.000	0.000	0.000

INTERIM TABLE Issued December 31, 1960.

TABLE III. - Concluded.

Aluminum (Al)

(Reference State)

0°K. to 932°K.	Solid
932°K. to 2736°K.	Liquid
2736°K. to 6000°K.	Ideal Gas Monatomic

For details see solid, liquid and ideal gas sheets.

TABLE IV - X-ray Diffraction Analysis of the Residue Resulting from the Reaction of the Tungsten Filament and the Aluminum Nitride Charge

Cu K α Radiation, Nickel Filter
 AlN Run #19
 Filament - Tungsten

<u>d (Å)</u>	<u>2θ</u>	<u>Intensity</u>	<u>Interpretation</u>
2.27	39.53	Weak	?
2.24	40.26	Very Strong	Tungsten
1.75	52.24	Very Weak	?
1.53	58.27	Strong	Tungsten
1.35	69.6	Very Weak	AlN
1.29	73.20	Strong	Tungsten

Table V - X-ray Diffraction Analysis of the Residue Resulting from the Reaction of the Rhenium Filament and the Aluminum Nitride Specimen

Cu K α Radiation, Nickel Filter
 AlN Run #17
 Filament - Rhenium

<u>d (Å)</u>	<u>2θ</u>	<u>Intensity</u>	<u>Interpretation</u>
2.70	33.15	Very Weak	AlN
2.37	37.93	Very Weak	AlN
2.226	40.49	Very Strong	Rhenium
2.105	42.93	Very Weak	Rhenium

TABLE VI - Analysis of Aluminum Nitride Heated on a Graphite Filament

Cu K α Radiation, Nickel Filter
AlN Run #6
Filament - Graphite

<u>d (Å)</u>	<u>2θ</u>	<u>Intensity</u>	<u>Interpretation</u>
2.70	33.15	Very Strong	AlN
2.49	36.04	Very Strong	AlN
2.37	37.93	Very Strong	AlN
1.83	49.78	Strong	AlN
1.56	59.18	Strong	AlN
1.41	66.22	Strong	AlN
1.35	69.6	Weak	AlN
1.32	71.40	Strong	AlN
1.30	72.67	Weak	AlN

TABLE VII- X-ray Diffraction Analysis of Aluminum Nitride Heated in a Tubular Graphite Filament

Cu K α Radiation, Nickel Filter
AlN Run #13
Filament - Graphite

<u>d (Å)</u>	<u>2θ</u>	<u>Intensity</u>	<u>Interpretation</u>
3.37	26.42	Very Weak	Graphite
2.70	33.15	Very Strong	AlN
2.49	36.04	Very Strong	AlN
2.37	37.93	Very Strong	AlN
1.83	49.78	Strong	AlN
1.56	59.18	Strong	AlN
1.41	66.22	Strong	AlN
1.35	69.60	Weak	AlN
1.32	71.40	Strong	AlN
1.30	72.67	Weak	AlN

TABLE VIII- X-ray Diffraction Analysis of Aluminum Nitride
Heated in a Tubular Graphite Filament

Cu K α Radiation, Nickel Filter
AlN Run #14
Filament - Graphite

<u>d (Å)</u>	<u>2θ</u>	<u>Intensity</u>	<u>Interpretation</u>
3.37	26.42	Very Weak	Graphite
2.70	33.15	Very Strong	AlN
2.49	36.04	Very Strong	AlN
2.37	37.93	Very Strong	AlN
1.83	49.78	Very Strong	AlN
1.56	59.18	Strong	AlN
1.41	66.22	Strong	AlN
1.35	69.6	Weak	AlN
1.32	71.40	Strong	AlN
1.30	72.67	Weak	AlN

TABLE IX - X-ray Diffraction Analysis of Aluminum Nitride
Melted in a Tubular Graphite Filament

Cu K α Radiation, Nickel Filter
AlN Run #20
Filament - Graphite

<u>d (Å)</u>	<u>2θ</u>	<u>Intensity</u>	<u>Interpretation</u>
3.37	26.42	Very Strong	Graphite
2.80	31.93	Very Weak	Al ₄ C ₃
2.70	33.15	Strong	AlN
2.49	36.04	Strong	AlN and/or Al ₄ C ₃
2.37	37.93	Strong	AlN
2.23	40.41	Very Weak	Al ₄ C ₃
1.83	49.78	Strong	AlN
1.56	59.18	Strong	AlN
1.41	66.22	Strong	AlN
1.35	69.6	Very Weak	AlN
1.32	71.40	Strong	AlN
1.30	72.67	Weak	AlN

TABLE X - X-ray Diffraction Analysis of Aluminum Nitride
Melted in a Tubular Graphite Filament

CuK α Radiation, Nickel Filter
AlN Run #21
Filament - Graphite

<u>d (Å)</u>	<u>2θ</u>	<u>Intensity</u>	<u>Interpretation</u>
3.37	26.42	Very Strong	Graphite
2.70	33.15	Strong	AlN
2.49	36.04	Strong	AlN
2.37	37.93	Strong	AlN
2.036	44.46	Very Weak	Graphite
1.83	49.78	Weak	AlN
1.682	54.51	Weak	Graphite
1.56	59.18	Strong	AlN
1.41	66.22	Strong	AlN
1.35	69.6	Very Weak	AlN
1.32	71.40	Weak	AlN
1.30	72.67	Very Weak	AlN

TABLE XI- X-ray Diffraction Analysis of Cerac Grade 1454
Aluminum Nitride Powder

<u>d (Å)</u>	<u>2θ</u>	<u>Intensity</u>	<u>Interpretation</u>
2.70	33.15	Very Strong	AlN
2.49	36.04	Very Strong	AlN
2.37	37.93	Very Strong	AlN
1.83	49.78	Strong	AlN
1.56	59.18	Strong	AlN
1.41	66.22	Strong	AlN
1.35	69.6	Weak	AlN
1.32	71.40	Strong	AlN
1.30	72.67	Weak	AlN